The Cyanobacterium *Spirulina platensis* Contains a Long Wavelength-Absorbing Pigment C_{738} (F_{760}^{77K}) at Room Temperature†

Birgit Koehne and Hans-Wilhelm Trissl*

Abteilung Biophysik, Fachbereich Biologie/Chemie, Universität Osnabrück, Barbarastrasse 11, D-49069 Osnabrück, FRG

Received November 6, 1997; Revised Manuscript Received January 22, 1998

ABSTRACT: *Spirulina platensis* is a cyanobacterium which usually lives under high-light conditions. Nonetheless, it is thought to contain the most red-shifted antenna pigment of all known Chl *a*-containing phototrophic organisms, as shown by its 77 K fluorescence peaking at 760 nm. To exclude preparation artifacts and to exclude the possibility that long wavelength-absorbing pigments form only when the temperature is lowered to 77 K, we carried out experiments with whole cells at room temperature. The combined analysis of stationary absorption and fluorescence spectra as well as fluorescence induction and time-resolved fluorescence decays shows that the pigment responsible for the 77 K fluorescence at 760 nm (i) has the oscillator strength of approximately one Chl *a* molecule, (ii) absorbs maximally at 738 nm (C_{738}^{293K}), (iii) is present only in the antenna system of PS I, (iv) participates in light collection, and (v) does not entail a low photochemical quantum yield. Other, more abundant but less red-shifted Chl *a* antenna pigments lead to a significantly larger absorption cross section of the photosynthetic unit of PS I above 700 nm compared to units that would not possess these long wavelength-absorbing pigments. These results support the hypothesis that the physiological role of long wavelength-absorbing pigments is to increase the absorption cross section at wavelengths of >700 nm when in densely populated mats the spectrally filtered light is relatively more intense at these wavelengths [Trissl, H.-W. (1993) *Photosynth. Res. 35,* 247−263].

The absorption maximum of the Q_y band of the bulk chlorophyll *a* (Chl *a*[1]), which is used for light collection in all oxygen-evolving organisms, is located at around 680 nm. As a consequence, the excited state in the light-harvesting complexes (LHC) is nearly isoenergetic with the primary donor, P680, of photosystem II (PS II) and any funnel effect is negligible. Nevertheless, rapid equilibration of the excited state and the high speed of the primary charge separation in the reaction center (RC) on the order of a few picoseconds establish a quantum yield of primary photochemistry of >80% (*1*). The presence of any antenna pigments absorbing at longer wavelengths than the bulk would diminish significantly the quantum yield.

The situation is different for photosystem I (PS I), where the red absorption maximum of the primary donor (P700) is located at 700 nm and funneling of the excitation energy toward the reaction center would be essential. However, in most systems studied, the main absorption band of the bulk Chl *a* in PS I is slightly red-shifted compared to that in PS II (*2*, *3*), which is due to so-called long wavelength-absorbing pigments in this antenna system. Some of them may have their Q_y band at much longer wavelengths than P700. These latter pigments necessarily reduce the maximal achievable quantum yield. The loss of quantum yield due to the presence of long wavelength-absorbing pigments depends critically on their number and the precise location of their absorption maxima (*4*). Of particular importance in this respect is the assessment of the red-most pigment since this determines the zero energy level in an antenna system, which in turn is needed to understand the physics of the trapping process.

The assay used most often to reveal the red-most pigments is fluorescence emission spectroscopy at low temperature (77 K), where the thermalization energy is no longer sufficient for repopulating higher states from the red-most form (*5*). At this temperature, excitons gather on the red-most pigments (instead of being trapped by the reaction center) and since they are normally not quenched the red-most pigments manifest themselves by their red-shifted fluorescence maxima. Fluorescence maxima at 77 K from different plants, algae, and cyanobacteria range from 690 to 760 nm, which shows that some PS I from the different species do not possess long wavelength-absorbing pigments. The largest red shift, F^{77K} = 760 nm, is found in the cyanobacterium *Spirulina platensis* (*6*). There is uncertainty about the absorption spectra of the pigments pertinent to the fluorescence at low temperatures. A pigment with an absorption maximum at 738 nm has been suggested to be present in PS I of maize (*7*).

The physiological relevance of these pigments is not clear. Different possibilities are under discussion. It has been suggested that they serve in focusing excitons close to the reaction center (*8*−*10*). Other authors think that they may

† This work was supported by the Deutsche Forschungsgemeinschaft (Grants SFB 171, TP-1, and GRK 174/3).

* To whom correspondence should be addressed.

[1] Abbreviations: Chl *a*, chlorophyll *a*; F_o, fluorescence with oxidized Q_A; F_m, fluorescence with reduced Q_A; LHC, light-harvesting complex; PS I, photosystem I; PS II, photosystem II; P680, primary donor of PS II; P700, primary donor of PS I; PSU, photosynthetic unit; Q_A, primary quinone acceptor of reaction center II; RC, reaction center.

S0006-2960(97)02750-5 CCC: $15.00
Published on Web 04/01/1998

have a protecting function (*11*) or are not involved in the light collection process (*12*). Further, it has been argued that they increase the absorption cross section of the photosynthetic unit (PSU) in the red (*4*).

There are two problems associated with elucidating the physiological and concomitantly the photophysical role of long wavelength-absorbing pigments in PS I. First, it is difficult to assess the absorption band of corresponding emitting pigments, C^{77K}, because of the unknown Stokes shift. Second, it is conceivable that these pigments may not be present at room temperature but may form only at low temperatures (*13, 14*). To solve these problems, the analysis of room-temperature data is obligatory.

We have selected *S. platensis* in our attempt to clarify the role of long wavelength-absorbing pigments because it contains the most red-shifted pigment of all known species. This should make it easier to arrive at definite conclusions. To exclude any preparation artifact, we performed most experiments with whole cells freshly harvested from the culture. The analysis of stationary fluorescence spectra at room temperature, fluorescence induction curves, spectral decomposition, and time-resolved fluorescence decay allowed us to separate the absorption and fluorescence spectra of PS II and PS I. These spectra obey the Stepanov relation derived for thermally equilibrated systems (*15, 16*). From this analysis, it can be concluded that under physiological conditions PS I of *S. platensis* contains a long wavelength-absorbing pigment absorbing at approximately 738 nm, which participates in the general light collection process.

MATERIALS AND METHODS

S. platensis [strain B 257.8 (*17*)] was obtained from the "Sammlung von Algenkulturen" at the University of Göttingen. The cells were grown photoautotrophically at 33 °C in the medium described by Schlösser et al. (*17*) under continuous light at an intensity of ≈0.7 mW cm^{-2} and aerated by sterile air. The cells were harvested after 12−14 days by centrifugation. Membrane fragments of *S. platensis* cells were prepared according to Kirilovsky et al. (*18*) with minor modifications. The Chl *a* concentration of membranes and whole cells was measured after extraction with 80% acetone/water (v/v) using the extinction coefficient given by Porra (*19*). Low-temperature fluorescence at 77 K of whole cells and membranes displayed a large peak at 760 nm, in agreement with published data (*6*).

Absorption spectra at room temperature were recorded with an Aminco DW-2000 spectrophotometer. Quantum-corrected fluorescence emission spectra were measured with a custom-built high-sensitivity flash fluorimeter. The excitation light was filtered through 441 or 620 nm narrow band interference filters (Schott), and the fluorescence was detected at 90° with respect to the exciting light in the wavelength range of 600−850 nm. The exciting flashes were sufficiently weak to allow for fluorescence spectra under conditions where all RCs were open (F_o, Q_A oxidized). Emission spectra with closed RCs (F_m, Q_A reduced) were measured after the addition of 20 μM DCMU [3-(3,4-dichlorophenyl)-1,1-dimethylurea] and with a preflash 100 μs before the exciting flash. For measurements with whole cells, the medium additionally contained 15% Ficoll to prevent sedimentation of the cells. For all measurements, the Chl *a* concentration of membranes was adjusted to 2 μM and that of whole cells to 5−7 μM.

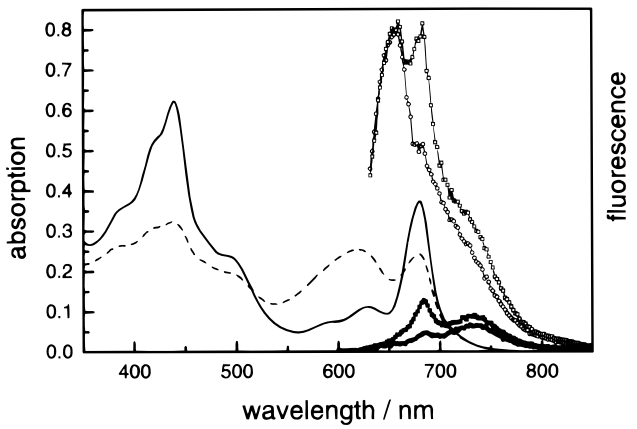

FIGURE 1: Absorption and fluorescence spectra of *S. platensis*. Absorption spectra of whole cells (dashed line) and membranes (solid line). Quantum-corrected fluorescence spectra of whole cells upon 620 nm excitation under F_o and F_m conditions (○ and □) and upon 441 nm excitation under F_o and F_m conditions (● and ■). The F_o spectra were obtained without addition of chemicals and the F_m spectra by addition of 20 μM DCMU and preillumination.

Measurements of the fluorescence decay kinetics in the picosecond time range were performed with a setup described before (*20*), and the data were analyzed as described by Wulf and Trissl (*21*). The excitation was performed at a repetition rate of 0.25 Hz with 30 ps laser flashes at 435.6 nm generated by a frequency-doubled Nd:YAG laser that produced an anti-Stokes Raman line of H_2.

RESULTS

An essential feature in this study was the study of the most intact system, namely, living cells. This, however, causes several experimental difficulties. A spectral decomposition of the absorption spectrum is hampered by light scattering and spectral flattening, and therefore, the fluorescence spectrum may be distorted by reabsorption due to the high pigment content of the cells. Furthermore, the overall fluorescence spectrum is a composite of the emission from phycobiliproteins and Chl *a* belonging to PS II and PS I. To a great extent, the following analysis is concerned with the separation of the corresponding spectral bands.

Stationary Spectra at Room Temperature. Figure 1 (dashed line) shows the absorption spectrum of whole cells of *S. platensis* corrected for light scattering by subtraction of a straight baseline that was adjusted to the original data at 800 nm. There are two peaks at >600 nm which can be assigned to phycobilisomes (620 nm) and Chl *a* (680 nm). The absorption spectrum of isolated membranes which was also corrected by a baseline subtraction (Figure 1, solid line) had only one dominating peak at 680 nm, indicating the loss of phycobilins. Both spectra were scaled to each other at the red absorption wing (720−760 nm), where the sieve effect is negligible. The higher peak height of the membranes at 680 nm compared to that of the cells indicates a significant sieve effect (*22*), which might scale down the fluorescence amplitudes at <720 nm due to reabsorption. However, in the region above 700 nm (which is the relevant wavelength range for our analysis), the spectra match very well.

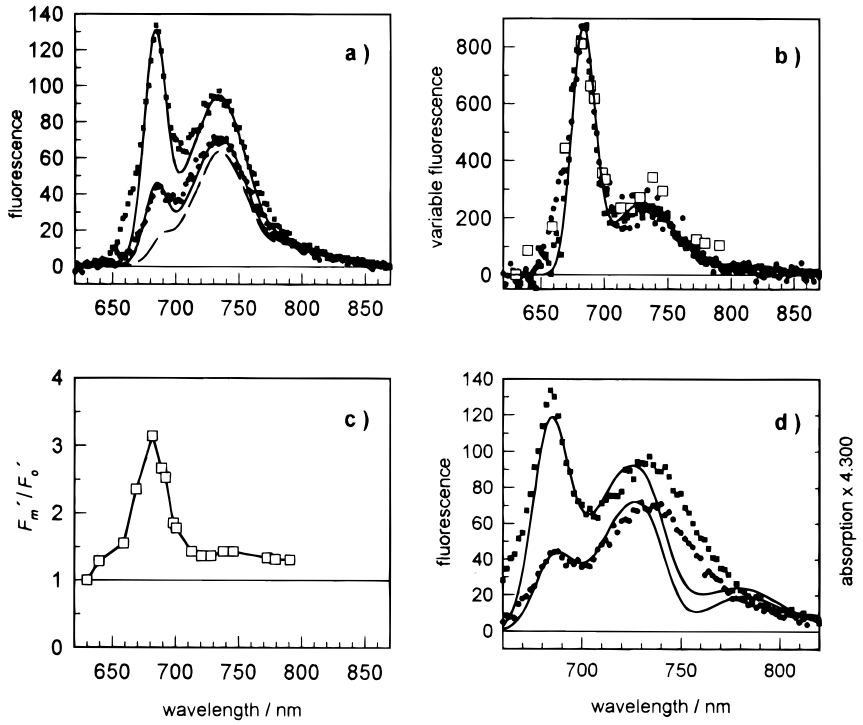

FIGURE 2: (a) Fluorescence spectra from Chl *a* under F_o and F_m conditions (● and ■) obtained from Figure 1 (whole cells, 441 nm excitation) by subtraction of the emission from phycobilisomes and their fits (solid lines) as described in the text. The contribution of PS I is shown as a dashed line. The dashed line represents the Stepanov transformation of the absorption spectrum of membranes as well as the Stepanov transformation of the PS I absorption spectrum (Figure 3). The latter two fluorescence spectra are indistinguishable in the presentation. (b) Variable fluorescence obtained as the difference of the fluorescence spectra under F_o and F_m conditions upon excitation at 620 nm (■) and 441 nm (●). Variable fluorescence (□) calculated from the induction measurement (Figure 2c) by means of eqs 2 and 3. Theoretical fit of the variable fluorescence by a Stepanov transformation of an assumed absorption spectrum (solid line). (c) Wavelength dependence of F'_m/F'_o from whole cells measured by fluorescence induction in the millisecond range upon excitation at 441 nm. The cells were dark-adapted for 10 min, and DCMU was added to 20 μM 3−5 min before the induction measurement. The excitation and emission wavelengths were selected by interference filters. (d) Fluorescence spectra from Chl *a* under F_o and F_m conditions (● and ■). Theoretical fluorescence spectra calculated from the PS I and PS II absorption spectra (Figure 3) by omitting the red-most pigment in PS I (solid lines).

The fluorescence spectra of whole cells of *S. platensis* upon excitation in the phycobilisomes (λ_{ex} = 620 nm) are shown in Figure 1 under F_o (open circles) and F_m conditions (open squares). The noisiness of our fluorescence spectra is due to the very low Chl concentration used to minimize reabsorption and to the very low excitation intensity to allow for F_o conditions. The F_o spectrum is very similar to that from isolated phycobilisomes (data not shown).

The fluorescence emission spectra obtained at a λ_{ex} of 620 nm are much higher than those at an excitation wavelength of 441 nm which excites predominantly Chl *a*. The two sets of fluorescence spectra were normalized to the photon fluences of the excitation source and the absorption of the sample at the respective excitation wavelengths. The much higher fluorescence yield upon phycobilisome excitation compared to Chl *a* excitation indicates that our cells contain a significant fraction of poorly connected phycobilisomes. This interpretation was confirmed by time-resolved fluorescence decay measurements (λ_{ex} = 532 nm) which showed major phases with time constants in the range of 400−800 ps (data not shown). The excitation wavelength of 620 nm is inappropriate for our investigation because it excites preferentially phycobilins which fluoresce with higher amplitudes than Chl *a* up to 800 nm. For this reason, we focus on 441 nm excitation, since we are interested in PS I fluorescence which is emitted by Chl *a* in the 700−800 nm region.

Spectral Separation of the Fluorescence Spectrum with Respect to PS I and PS II. To obtain pure fluorescence spectra from Chl *a*, we subtracted from the 441 nm excited fluorescence spectra (Figure 1, F_o, filled circles; and F_m, filled squares) the fluorescence spectrum of phycobilisomes so that the resulting fluorescence at 650 nm became zero. The corresponding F_o and F_m spectra are shown in Figure 2a (circles and squares). The spectral separation of the Chl *a* fluorescence with respect to PS II and PS I can be achieved through identifying the PS II fluorescence by its variable fluorescence ($F_v = F_m - F_o$). The variable fluorescence obtained by subtracting the F_o and F_m spectra excited at 441 nm (Figure 2a) and excited at 620 nm is shown in Figure 2b (filled circles and filled squares, respectively). Before their subtraction, the 620 nm data in Figure 1 were scaled to each other to yield the same amplitude at 650 nm and then adjusted to the 441 nm data.

The variable fluorescence spectrum is solely due to PS II. It displays a dominant peak at 683 nm with a smaller broad satellite band at 720−760 nm, which corresponds to the usual vibrational bands of chlorophyll emission. The spectrum resembles closely those reported for PS II (*23*). The absence of large peaks at >700 nm clearly indicates that this photosystem does not possess long wavelength-absorbing pigments.

Stepanov Relation. To test if the fluorescence originates from thermally equilibrated antenna systems, we applied to

Table 1: Spectral Decomposition of PS II with Gaussian Functions and the Exciton Distribution According to a Boltzmann Equilibrium[a]

λ_{max} (nm)	$N_i^{PS\ II}$	exciton occupancy
655	9.42	0.018
676	33.10	0.632
683	2.2	0.083
709	0.17	0.099
725	0.023	0.167
745	0.002	0.000

[a] The total number of Chl *a* pigment molecules in a photosynthetic unit ($N^{PS\ II}$) was assumed to be 45. The space separates intense bands that can be associated with real existing chromophores ($N > 1$) from bands that represent minor electronic transitions belonging to the chromophores.

our data the Stepanov relation (*15*, *16*), which correlates the absorption, $A(\nu)$, and the spectral density of the fluorescence quantum yield, $F(\nu)$, for thermalized systems. On a frequency scale, ν, the two spectra are related by

$$F(\nu) \sim \nu^3 e^{(-h\nu/k_B T)} A(\nu) \quad (1)$$

where h is Planck's constant, k_B the Boltzmann constant, and T the temperature. The equation allows one to calculate absorption spectra from fluorescence spectra and vice versa. For the practical application of this formula for fluorescence spectra, see Dau and Sauer (*24*).

First, we took the absorption spectrum of membranes (Figure 1, solid curve), fitted the red part (660−800 nm) with Gaussian bands (not shown), and calculated a Stepanov-transformed fluorescence spectrum (Figure 2a, dashed line). We also transformed the original absorption data and found a similar fluorescence spectrum for wavelengths of <740 nm (not shown). For wavelengths of >740 nm, the calculated fluorescence spectrum becomes undefined due to small noise in the absorption spectrum. The spectrum shows a dominant maximum in the red at 735 nm and a shoulder at 685 nm. The large deviations from the measured fluorescence around 690 nm (Figure 2a) demonstrate that the system is not thermally equilibrated. The most simple explanation then is to assume that the sample contains two thermalized systems. These may be PS I and PS II, since for both photosystems the validity of eq 1 has been shown (*7*, *24*, *25*). If the red part of the absorption is ascribed to PS I only, then the peak at 735 nm and the shoulder at 685 nm should belong to the same thermally equilibrated system, i.e., PS I.

Second, we constructed a hypothetical PS II absorption spectrum with Gaussian bands (using their widths and relative heights as fit parameters; Table 1) which were subsequently Stepanov-transformed yielding noise-free calculated fluorescence spectra. The best fit of the variable fluorescence is shown in Figure 2b (solid line). The PS II absorption spectrum displays a high precision for wavelengths of >680 nm (relevant for the conclusions of our paper) and low precision for wavelengths of <680 nm (this wavelength range does not contain relevant information on the long wavelength-absorbing pigments).

To begin with the further analysis, we neglect distortions by fluorescence reabsorption. The above procedure yielded the shape of the PS II absorption spectrum but not its amplitude. In any case, the PS I absorption spectrum should

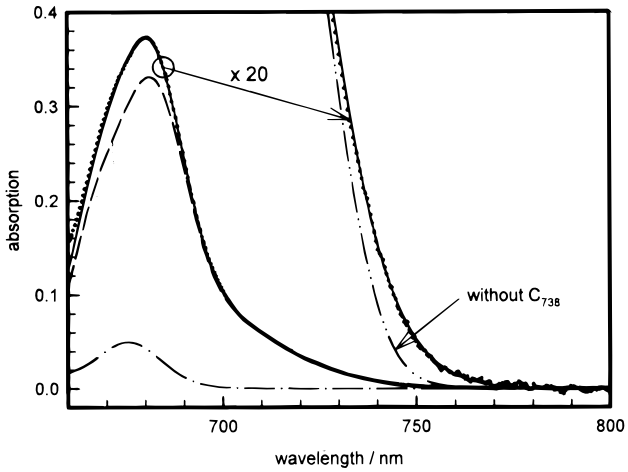

FIGURE 3: Absorption spectrum of membranes (dots) and its description by a sum of Gaussian bands (solid line). Parameters are listed in Table 1. Decomposition of this spectrum with respect to PS I (dash) and PS II (dash−dot). To illustrate the quality of the theoretical description of the measured absorption spectrum in the very red, the same data were amplified 20 times as indicated. Theoretical absorption spectrum in which the red-most pigment is ommited (dash−dot−dot line).

be the difference between the measured spectrum and the PS II absorption spectrum. Alternatively, it could be conceivable that a third pigment group containing long wavelength-absorbing pigments exists. To obtain the relative amplitudes of PS II absorption and the remaining absorption, which is essentially PS I, we set the integrated areas of the PS II and non-PS II absorption spectra in proportion to their Chl *a* antenna sizes and their stoichiometric ratio. Taking the antenna sizes $N^{PS\ I}$ and $N^{PS\ II}$ to be 100 and 45, respectively, and assuming the stoichiometric ratio PS I/PS II = 4 (*26*) yield the spectral decompositon of the absorption spectrum with respect to PS I and PS II shown in Figure 3 (dashed and dash−dot curves, respectively). From these decomposed PS II and PS I absorption spectra, one can calculate in principle the Stepanov-transformed fluorescence spectra of PS II and PS I and test whether the sum of both agrees with the experimental one (see below).

We also inspected the influence of fluorescence reabsorption artifacts in whole cells. The fluorescence spectra of whole cells and membranes at equal chlorophyll concentrations showed an approximately 2-fold higher fluorescence intensity at 685 nm (relative to the 735 nm peak) in membranes compared to whole cells. The analysis with this higher 685 nm fluorescence resulted in an approximately 2-fold lower PS I/PS II stoichiometric ratio, but left the shapes of the decomposed PS I and PS II spectra nearly unchanged. It is worth mentioning that lower PS I/PS II stoichiometries are also consistent with the current literature (*27*−*29*) and our final conclusions are not dependent on the exact numerical value.

Third, we attempted to describe quantitatively the Chl *a* fluorescence spectra under F_o and F_m conditions by summing up fluorescence spectra calculated from the decomposed absorption spectrum (see above) by means of the Stepanov relation. For this operation, the fluorescence quantum yields are needed. These were obtained from the experimentally determined time constant of 70 ± 8 ps for the main phase in the time-resolved fluorescence decay, yielding for PS I a

$\Phi^{PS\ I}$ of 0.005 (see below) and taking the fluorescence yield of PS II in the open state $\Phi_f^{PS\ II(o)}$ to be 0.012 (*30*) and in the closed state $\Phi_f^{PS\ II(c)}$ to be 0.044 to fulfill $F_m/F_o = 3.7$. Summing up the PS I and PS II fluorescence spectra calculated from the decomposed absorption spectrum by means of the Stepanov relation (each normalized to the integrated area of 1) according to their yields and their stoichiometric ratio gives the solid lines through the data points (Figure 2a). The good fit of the calculated and measured fluorescence spectra demonstrates that a two-compartment system is sufficient to describe the data. There is no need to assume a further pigment pool.

To exclude the possibility that the stationary fluorescence spectra under F_o and F_m conditions and the resulting spectrum of the variable fluorescence were distorted by state transitions, which may occur on the time scale of seconds to minutes (*31*), we performed fluorescence induction measurements of dark-adapted cells in the millisecond time range, using a xenon flash technique (*32*). *S. platensis* cells were excited at 441 nm, and the induction was measured at different emission wavelengths. The corresponding F_m/F_o as a function of the wavelength is shown in Figure 2c.

To extract the mere PS II contribution, $F_o^{PS\ II}(\lambda)$ and $F_m^{PS\ II}(\lambda)$, to the fluorescence yields in the fluorescence induction measurements, one can utilize the fact that the PS I fluorescence yield, $\int F^{PS\ I}(\lambda)\ d\lambda$, is constant. Then the measured fluorescence intensities, $F'_o(\lambda)$ and $F'_m(\lambda)$, under F_o and F_m conditions are

$$F'_o(\lambda) = F^{PS\ I}(\lambda) + F_o^{PS\ II}(\lambda) \quad (2a)$$

$$F'_m(\lambda) = F^{PS\ I}(\lambda) + F_m^{PS\ II}(\lambda) \quad (2b)$$

The variable fluorescence $F_v^{PS\ II} = F_m^{PS\ II} - F_o^{PS\ II}$ is independent of $F^{PS\ I}$. For the relation between the wavelength-dependent measured $F'_m(\lambda)/F'_o(\lambda)$ and the wavelength-independent $F_m^{PS\ II}/F_o^{PS\ II}$, one obtains for the PS I contribution

$$F^{PS\ I}(\lambda) = \frac{(F_m^{PS\ II}/F_o^{PS\ II})F'_o(\lambda) - F'_m(\lambda)}{(F_m^{PS\ II}/F_o^{PS\ II}) - 1} \quad (3)$$

in which $F_m^{PS\ II}/F_o^{PS\ II}$ is an a priori unknown number. However, the range of possible values is rather confined by the given experimental data. The ratio being sought must not be smaller than the maximal measured value (3.2), and it cannot be larger than a maximal value which is given when the theoretical PS I fluorescence spectra adopt negative amplitudes at any wavelength. From these conditions, we obtain $3.2 \leq F_m^{PS\ II}/F_o^{PS\ II} \leq 4$. Taking $F_m^{PS\ II}/F_o^{PS\ II} = 3.7$ and the fluorescence spectrum of PS I (Figure 2a, dashed curve), we calculate from the data in Figure 2c the variable fluorescence due to millisecond induction measurements shown in Figure 2b (□). Within the experimental error, all spectra are the same and agree with typical PS II fluorescence spectra from higher plants (*23*).

Pigment Composition. The above spectral decomposition of the absorption spectrum with respect to PS I and PS II by Gaussian bands allows us to estimate the approximate number of pigments contained in the spectral sub-bands of a PSU. These are obtained by setting the area under the PS I and PS II bands in relation to the antenna sizes (Table 1).

Table 2: Spectral Decomposition of PS I with Gaussian Functions and the Exciton Distribution According to a Boltzmann Equilibrium[a]

λ_{max} (nm)	$N_i^{PS\ I}$	exciton occupancy
667	40.75	0.011
683	76.71	0.098
701	12.07	0.015
713	7.91	0.212
726	2.24	0.206
737.6	1.04	0.275
760	0.04	0.076
780	0.002	0.024

[a] The total number of Chl *a* pigment molecules in a photosynthetic unit ($N^{PS\ I}$) was assumed to be 100. The space separates intense bands that can be associated with real existing chromophores ($N > 1$) from bands that represent minor electronic transitions belonging to the chromophores.

It is obvious that PS II lacks pigments absorbing at >683 nm. In PS I, however, there is a significant number of pigments absorbing at >700 nm (Table 2). The red-most one is located at approximately 738 ± 1 nm (C_{738}^{293K}). To substantiate its relevance for the analysis, we omitted tentatively this red-most pigment. This leads to a significant deviation from the absorption spectrum (Figure 3, dash−dot−dot line) and a drastic deviation at 755 nm of the calculated fluorescence spectrum from the measured ones (Figure 2d, solid lines). Alternatively, when the C_{738}^{293K} is not omitted, the absorption spectrum is well described, irrespective of whether it is excitonically connected to other antenna pigments. One can then calculate the cases where it is decoupled from the general antenna system assuming that it is either perfectly quenched or nonquenched (3 ns losses). The fluorescence spectrum in the perfectly quenched case agrees with Figure 2d (solid lines), and in the non-quenched case, strong deviations to the opposite side of the measured fluorescence spectrum occur. This shows that the fluorescence yield of C_{738}^{293K} is the same as the average fluorescence yield of PS I. Further model calculations which assume two pigments at 738 nm instead of one show strong deviations from the measured absorption and fluorescence spectra. These calculations establish the existence of one pigment absorbing at 738 nm (C_{738}^{293K}) that participates at room temperature in the collective antenna system of PS I in *S. platensis*.

Fluorescence Decay Kinetics. To obtain information on the trapping time of PS I, whole cells and membranes were excited with 30 ps flashes at 435.6 nm. Under F_o and F_m conditions in the wavelength region between 720 and 750 nm, there was a dominant phase (>90%) of 70 ± 8 ps, which did not depend on the redox conditions (data not shown). This phase is therefore ascribed to trapping in PS I. A similar phase has been reported for PS I trimers in membranes from *S. platensis* (*14*).

Growth Conditions. To inspect whether the presence of long wavelength pigments is an inherent property of the cyanobacterium *S. platensis*, the light intensitiy was reduced 5-fold and in another batch the nitrate content in the medium was reduced 10-fold. In both cases, the 77 K fluorescence spectra displayed the strong 760 nm peak. We also converted the cells into state 1 by illumination with light of >715 nm (RG 715) for 15 min before and during the recording of a

fluorescence spectrum and observed the same room-temperature spectra as from cells in state 2 (the usual dark-adapted conditions). Obviously, the presence of far-red pigments in *S. platensis* is an intrinsic feature of this organism, invariant of growth conditions, light quality, and state transitions.

DISCUSSION

Energy transfer from PS II to PS I in cyanobacteria (spillover) is often thought to be an important process. The characteristic long wavelength emission of PS I in *S. platensis* at room temperature brings about the possibility of judging the significance of this effect. If spillover would occur, the PS II fluorescence emission spectrum (Figure 2b) should show an intense band at 735 nm similar to that of PS I. However, this is not the case. The relative peak heights of the PS II emission at 683 and 735 nm (Figure 2b) are very similar to those of Chl *a* in solvents (*33*) or PS II of higher plants (*23*), and therefore, a significant spillover in this cyanobacterium can be excluded. Both photosystems appear to be excitonically well separated as suggested previously (*34*).

In this study, we applied a new spectroscopic concept to separate the two photosystems. It is based on the experimentally accessible total absorption spectrum (PS I and PS II), the total fluorescence spectra (PS I and PS II), the spectrum of variable fluorescence (PS II only), and the assumption of thermal equilibration in each of the two photosystems. The pure PS II fluorescence spectrum is then utilized to separate the total absorption spectrum and total fluorescence spectrum with respect to PS I and PS II. The procedure is to obtain the PS II absorption spectrum from its fluorescence spectrum. The PS I absorption spectrum is then obtained as the difference to the total absorption spectrum (assuming a PS I/PS II stoichiometric ratio). If these two absorption spectra belong to equilibrated pigment pools, then their fluorescence spectra are predictable. With the knowledge of the fluorescence yields, the total fluorescence spectrum can be calculated in succession. The agreement or disagreement of this calculated fluorescence spectrum with the measured one indicates that either (i) only the two pigment pools of PS I and PS II are involved or (ii) additional unconnected pigment pools exist.

A comparison of the PS II and PS I absorption spectra (Figure 3) illustrates the much larger Chl *a* absorption cross section of PS I compared to that of PS II. Yet a balanced linear electron flow can be realized owing to the additional energy supply of PS II by the phycobilisomes.

The decomposition of the absorption spectrum of *S. platensis* membranes with Gaussians and the weighting of their area with the antenna sizes of PS II and PS I and with the PS I/PS II stoichiometric ratio (Figure 3) allowed us to determine that the red-most band is equivalent to one chromophore, C_{738}^{293K} (Table 1). This suggests that the extreme bathochromic shift of C_{738}^{293K} may originate from protein−chromophore interactions. Alternatively, the spectral shift may also be caused by chromophore−chromophore interaction as suggested by Karapetyan et al. (*14*) or dimer formation (*35*) if part of the oscillator strength would occur at shorter wavelengths.

Although the red-most antenna pigment C_{738}^{293K} lies energetically very low (3.6 k_BT below P700 at room temperature), it does not act as a trap but is part of a thermally equilibrated antenna system as shown by the validity of the Stepanov relation and a relative exciton occupancy of 0.3 as calculated from the Boltzmann distribution (Table 2). The more abundant, less red-shifted pigments at 713 nm carry a comparable high exciton concentration.

Given our spectral decomposition of PS I (Table 2), a fluorescence decay kinetics of 70 ps, and thermal equilibration, a lower limit for the rate constant of the primary charge separation in the naked PS I reaction center k_p of $\geq$(0.64 ps)$^{-1}$ can be estimated, in agreement with Jennings et al. (*36*). Hence, the primary photochemistry seems to be even faster than estimates from other studies (*7*, *37*, *38*).

The astonishingly far red-shifted red-most antenna pigment in *S. platensis* has obviously no dramatic effect on the yield of the primary photochemistry. The overall trapping time of approximately 70 ps is comparable to that of higher plants and allows for yields still higher than 95%. From the analysis of time-resolved fluorescence on PS I trimeric particles, Karapetyan et al. (*14*) suggest a 30 ps trapping time as found in other cyanobacteria. If this should be true, the primary charge separation should be 3 times faster; i.e., $k_p \geq$ (275 fs)$^{-1}$.

In conclusion, long wavelength-absorbing pigments in PS I, even when they lie 38 nm more to the red than the primary donor P700 as in *S. platensis* or in maize (*7*), do not represent any enigma from the photophysical point of view. Therefore, one only has to deal with its physiological role to understand their presence. One of the authors has suggested that their purpose is to increase the absorption cross section of the PSU under living conditions where 680 nm light is filtered out by other Chl *a*-containing cells, thus producing light intensities that are relatively more intense at >700 nm than at 680 nm (*4*). Exactly this happens in the case of *S. platensis* since, although it is a typical high-light organism living in well-illuminated alkaline lakes (*39*), it grows to high cell densities which bring about the above-mentioned light conditions for cells living in greater depths. It is worth mentioning that, due to turbulence in the water layers, cells from the surface may be circulated to these red-enhanced light conditions. All cells of a living community are prepared for this situation because the amount and composition of the long wavelength-absorbing pigments in *S. platensis* does not depend on the growth conditions as shown in this study.

ACKNOWLEDGMENT

The authors thank Dr. J. Breton and Dr. W. Leibl for borrowing for us the H_2 Raman shifter, Dr. R. C. Jennings for helpful discussions, and Prof. W. Junge for his interest and support of this work.

REFERENCES

1. Schatz, G. H., Brock, H., and Holzwarth, A. R. (1988) *Biophys. J. 54*, 397−405.
2. Müller, A., Rumberg, B., and Witt, H. T. (1963) *Proc. R. Soc. London, Ser. B. 157*, 313.
3. Ried, A. (1972) in *Proceedings of the 2nd International Congress on Photosynthesis* (Forti, G., Avron, M., and Melandri, A., Eds.) pp 763−772.
4. Trissl, H.-W. (1993) *Photosynth. Res. 35*, 247−263.
5. Brody, S. S. (1958) *Science 128*, 838−839.
6. Shubin, V. V., Murthy, S. D. S., Karapetyan, N. V., and Mohanty, P. S. (1991) *Biochim. Biophys. Acta 1060*, 28−36.

7. Croce, R., Zucchelli, G., Garlaschi, F. M., Bassi, R., and Jennings, R. C. (1996) *Biochemistry 35*, 8572−8579.
8. van Grondelle, R., and Sundström, V. (1988) in *Excitation energy transfer in photosynthesis*, *Photosynthetic Light-Harvesting Systems. Organization and Function* (Scheer, H., and Schneider, S., Eds.) pp 403−438, de Gruyter, Berlin and New York.
9. Mukerji, I., and Sauer, K. (1990) in *A spectroscopic study of a photosystem I antenna complex*, *Current Research in Photosynthesis* (Baltscheffsky, M., Ed.) pp 321−324, Kluwer, Dordrecht, The Netherlands.
10. Jia, Y., Jean, J. M., Werst, M. M., Chan, C.-K., and Fleming, G. R. (1992) *Biophys. J. 63*, 259−273.
11. Mukerji, I., and Sauer, K. (1989) in *Temperature-dependent steady-state and picosecond kinetic fluorescence measurements of a photosystem I preparation from spinach*, *Photosynthesis* (Briggs, W. R., Ed.) pp 105−122, Alan R. Liss, Inc., New York.
12. van der Lee, J., Bald, D., Kwa, S. L. S., van Grondelle, R., Rögner, M., and Dekker, J. P. (1993) *Photosynth. Res. 35*, 311−321.
13. Satoh, K., and Butler, W. L. (1978) *Biochim. Biophys. Acta 502*, 103−110.
14. Karapetyan, N. V., Dorra, D., Schweitzer, G., Bezsmertnaya, I. N., and Holzwarth, A. R. (1997) *Biochemistry 36*, 13830.
15. Stepanov, B. I. (1957) *Sov. Phys. Dokl. 2*, 81−84.
16. Dau, H. (1996) *Photosynth. Res. 48*, 139−145.
17. Schlösser, U. G. (1994) *Bot. Acta 107*, 113−186.
18. Kirilovsky, D. L., Boussac, A. G. P., van Mieghem, F. J. E., Ducruet, J. M. R. C., Sétif, P., Yu, J. J., Vermaas, W. F. J., and Rutherford, A. W. (1992) *Biochemistry 31*, 2099−2107.
19. Porra, R. J., Thompson, W. A., and Kriedemann, P. E. (1989) *Biochim. Biophys. Acta 975*, 384−394.
20. Trissl, H.-W., and Wulf, K. (1995) *Biospectroscopy 1*, 71−82.
21. Wulf, K., and Trissl, H.-W. (1995) *Biospectroscopy 1*, 55−69.
22. Duysens, L. N. M. (1956) *Biochim. Biophys. Acta 19*, 1−12.
23. Jennings, R. C., Garlaschi, F. M., Bassi, R., Zucchelli, G., Vianelli, A., and Dainese, P. (1993) *Biochim. Biophys. Acta 1183*, 194−200.
24. Dau, H., and Sauer, K. (1996) *Biochim. Biophys. Acta 1273*, 175−190.
25. Zucchelli, G., Garlaschi, F. M., Croce, R., Bassi, R., and Jennings, R. C. (1995) *Biochim. Biophys. Acta 1229*, 59−63.
26. Shubin, V. V., Tsuprun, V. L., Bezsmertnaya, I. N., and Karapetyan, N. V. (1993) *FEBS Lett. 334*, 79−82.
27. Kobayashi, M., Watanabe, T., Nakazato, M., Ikegami, I., Hiyama, T., Matsunaga, T., and Murata, N. (1988) *Biochim. Biophys. Acta 936*, 81−89.
28. Melis, A., and Brown, J. S. (1980) *Proc. Natl. Acad. Sci. U.S.A. 77*, 4712−4716.
29. Schluchter, W. M., Shen, G. H., Zhao, J. D., and Bryant, D. A. (1996) *Photochem. Photobiol. 64*, 53−66.
30. Schatz, G. H., Brock, H., and Holzwarth, A. R. (1987) *Proc. Natl. Acad. Sci. U.S.A. 84*, 8414−8418.
31. Fujita, Y., Murakami, A., Aizawa, K., and Ohki, K. (1994) in *Short-term and long-term Adaptation of the photosynthetic apparatus: Homeostatic properties of thylakoids*, *The Molecular Biology of Cyanobacteria* (Bryant, D. A., Ed.) pp 677−692, Kluwer, Dordrecht, The Netherlands.
32. Trissl, H.-W. (1996) *Photosynth. Res. 47*, 175−185.
33. Belanger, D., Leblanc, R. M., and Kurucsev, T. (1992) *Photochem. Photobiol. 55*, 887−894.
34. Trissl, H.-W., and Wilhelm, C. (1993) *Trends Biochem. Sci. 18*, 415−419.
35. Gobets, B., van Amerongen, H., Monshouwer, R., Kruip, J., Rögner, M., van Grondelle, R., and Dekker, J. P. (1994) *Biochim. Biophys. Acta 1188*, 75−85.
36. Jennings, R. C., Zucchelli, G., Croce, R., Valkunas, L., Finzi, L., and Garlaschi, F. M. (1997) *Photosynth. Res. 52*, 245−253.
37. Dimagno, L., Chan, C. K., Jia, Y. W., Lang, M. J., Newman, J. R., Mets, L., Fleming, G. R., and Haselkorn, R. (1995) *Proc. Natl. Acad. Sci. U.S.A. 92*, 2715−2719.
38. Hastings, G., Kleinherenbrink, F. A. M., Lin, S., and Blankenship, R. E. (1994) *Biochemistry 33*, 3185−3192.
39. Ciferri, O. (1983) *Microbiol. Rev. 47*, 551−578.

BI9727500